

# Assessing non-Gaussian quantum state conversion with the stellar rank

Oliver Hahn<sup>1,2</sup>, Giulia Ferrini<sup>2</sup>, Alessandro Ferraro<sup>3,4</sup>, and Ulysse Chabaud<sup>5</sup>

<sup>1</sup>Department of Basic Science, The University of Tokyo, 3-8-1 Komaba, Meguro-ku, Tokyo, 153-8902, Japan

<sup>2</sup>Wallenberg Centre for Quantum Technology, Department of Microtechnology and Nanoscience, Chalmers University of Technology, Sweden , SE-412 96 Göteborg, Sweden

<sup>3</sup>Dipartimento di Fisica “Aldo Pontremoli”, Università degli Studi di Milano, I-20133 Milano, Italy

<sup>4</sup>Centre for Theoretical Atomic, Molecular and Optical Physics, Queen’s University Belfast, Belfast BT7 1NN, United Kingdom

<sup>5</sup>DIENS, École Normale Supérieure, PSL University, CNRS, INRIA, 45 rue d’Ulm, Paris, 75005, France

**State conversion is a fundamental task in quantum information processing. Quantum resource theories allow to analyze and bound conversions that use restricted sets of operations. In the context of continuous-variable systems, state conversions restricted to Gaussian operations are crucial for both fundamental and practical reasons — particularly in state preparation and quantum computing with bosonic codes. However, previous analysis did not consider the relevant case of approximate state conversion. In this work, we introduce a framework for assessing approximate Gaussian state conversion by extending the stellar rank to the approximate stellar rank, which serves as an operational measure of non-Gaussianity. We derive bounds for Gaussian state conversion under both approximate and probabilistic conditions, yielding new no-go results for non-Gaussian state preparation and enabling a reliable assessment of the performance of generic Gaussian conversion protocols.**

## 1 Introduction

Understanding the boundaries between quantum computing architectures that are capable of providing quantum advantage for computation from those which are not is of crucial importance for the design of useful quantum computers. A tool to develop this understanding is the use of resource theories [1]. In this framework, a set of [ulysses.chabaud@inria.fr](mailto:ulysses.chabaud@inria.fr)

states, operations and measurements is designed to be “free”. Often, this notion corresponds to the ease in the experimental capability of implementing such circuits elements. For notable examples, theorems have been derived that restrict the power of architectures made of solely free states, operations and measurements. Quantum computers over continuous variable (CV) systems [2–6], where information is encoded via bosonic codes [7–12], have emerged as an alternative to the ones based on two-level systems. In the context of these systems, a paradigmatic divide between “free” and “resourceful” circuit elements is the one between Gaussian [13, 14] and non-Gaussian [15] circuit elements. Gaussian operations are generally regarded as easier to achieve experimentally, in particular with optical set-ups [4, 14]. At the same time, circuits that are solely based on Gaussian elements are classically efficiently simulatable, i.e., they cannot provide exponential speed up for computation [16]. This result has also been extended to incorporate further simulatable architectures based on quasi-probability distributions; for instance circuits where the Wigner function is non-negative everywhere are simulatable [17–20]. In this scenario, non-Gaussian states emerge as necessary resources for implementing universal quantum computation based on CV systems [15].

The framework of resource theories is instrumental to characterize the convertibility between resourceful states by means of free operations. It is indeed still an open question which non-Gaussian states actually provide quantum advantage for computation when supplied to Gaussian (simulatable) architectures. Therefore, showing the convertibility of non-Gaussian states to

known resource states that unlock computational universality is a relevant way to assess the actual resourcefulness of general non-Gaussian states. Moreover, if some non-Gaussian quantum states can be prepared experimentally and Gaussian operations are easier to achieve, Gaussian conversion may unlock the ability of preparing new non-Gaussian quantum states in the lab; hence, characterizing convertibility of non-Gaussian states is useful for quantum state preparation. Such characterization can be achieved by identifying suitable measures of resourcefulness, i.e., monotones quantifying the amount of resourcefulness of a state, and by deriving bounds that constrain the convertibility of states with different amount of resourcefulness.

Various measures and indicators of non-Gaussianity have been proposed so far [15]. These includes negativity of the Wigner function, or Wigner negativity for short [21–23], stellar rank [24, 25] or  $n$ -photon genuine quantum non-Gaussianity [26], Gaussian rank and Gaussian extent [27]. For the case of Wigner negativity, a resource theory has been developed, which allows for deriving bounds restricting which exact state conversions are in principle possible [22, 23].

However, all the bounds that were derived so far do not take into account the experimentally relevant case of approximate state conversion, where we wish to convert a resourceful state into another resourceful state approximately, i.e., up to a certain value of suitable measures of similarity such as fidelity or trace distance.

In this work, we close this gap and introduce a general framework for assessing Gaussian state conversion in the approximate setting. To achieve this, we generalise the stellar rank [24, 25] and introduce the notion of  $\epsilon$ -approximate stellar rank of a state  $\rho$ , as the minimum stellar rank of states that are  $\epsilon$ -close to  $\rho$  in fidelity. We demonstrate that the  $\epsilon$ -approximate stellar rank is a valid measure of non-Gaussianity, i.e., that it satisfies all properties required for being a monotone. Based on this new measure of non-Gaussianity, for a given precision  $\delta > 0$ , we provide a  $\epsilon$ -parameterized family of bounds that, when simultaneously satisfied, indicate potential convertibility between non-Gaussian states, while when violated for any single value of the parameter  $\epsilon$  rule out the possibility of approximate Gaussian convertibility of the input to the target state within

trace distance less or equal to  $\delta$ . We illustrate this machinery on a pedagogical example, the Gaussian conversion from Fock state  $|2\rangle$  to  $|1\rangle \otimes |1\rangle$ . Based on these conversion bounds, we assess the efficiency of Gaussian conversion protocols that were previously studied in the literature [28, 29]. For the specific case of the conversion from a trisqueezed state to a cubic phase state studied in [28], we show that the bounds we derive are fairly tight; conversely, our analysis proves near optimality the experimentally relevant protocol proposed in [28]. Importantly, we show that the  $\epsilon$ -approximate stellar rank can be computed efficiently in most relevant cases. Our framework allows to study and meaningfully assess Gaussian conversion protocols, which are instrumental for non-Gaussian quantum state preparation and quantum computing with bosonic systems.

The paper is structured as follows. In section 2, we provide some background on resource theories and continuous-variable quantum information theory, including the stellar rank. In section 3, we introduce formally the approximate stellar rank, demonstrate its main properties and explain how it can be computed. In section 4, we use this new non-Gaussianity measure to derive Gaussian conversion bounds, applicable to exact, approximate, deterministic and probabilistic protocols; we further use these bounds to obtain new no-go results for Gaussian conversion. In section 5, we present applications of these bounds for assessing the quality of existing Gaussian conversion protocols; we conclude in section 6.

## 2 Background

### 2.1 Resource theories

In this section we provide a brief review of resource theories and refer the reader to [1, 22] for further details.

A resource theory is characterized by a set of free states  $\mathcal{G}$  and a set of free operations  $\mathcal{F}$ . The set of free states is closed under the action of free operations, namely it holds for  $\forall g \in \mathcal{G}$  that  $\Lambda(g) \in \mathcal{G}, \forall \Lambda \in \mathcal{F}$ . Every state not contained in the set of free states  $\mathcal{G}$  is called a *resource*. Resource monotones have been introduced to quantify the resource content of a state.

**Definition 1** (Resource monotone). *A mapping  $\mathcal{M}$  from the set of all states to the real num-*

bers is called a resource monotone, if it is non-increasing under the set of free operations  $\mathcal{F}$ , i.e.,  $\forall \rho \in \mathcal{H}$ ,

$$\mathcal{M}(\rho) \geq \mathcal{M}(\Lambda(\rho)), \quad \forall \Lambda \in \mathcal{F}. \quad (1)$$

Monotones in the literature do not fulfill necessarily all properties listed below, but they are useful in their own right and are used in this manuscript.

**Definition 2** (Faithfulness). A monotone is called faithful if there is a constant  $c \in \mathbb{R}$  such that  $\mathcal{M}(\rho) = c, \forall \rho \in \mathcal{G}$  and  $\mathcal{M}(\rho) > c$  otherwise.

The most common conventions is either  $c = 0$  if the monotone is (sub-)additive and  $c = 1$  if the monotone is (sub-)multiplicative.

**Definition 3** (Additivity and sub-additivity). A monotone  $\mathcal{M}$  is called additive if

$$\mathcal{M}(\rho \otimes \sigma) = \mathcal{M}(\rho) + \mathcal{M}(\sigma). \quad (2)$$

A monotone  $\mathcal{M}$  is called sub-additive if

$$\mathcal{M}(\rho \otimes \sigma) \leq \mathcal{M}(\rho) + \mathcal{M}(\sigma). \quad (3)$$

(Sub-)additivity is a very useful property, since it ensure that preparing a free state in an auxiliary system does not increase the resource amount.

**Definition 4** (Monotonicity on average (ideal)). A monotone  $\mathcal{M}$  is called monotone on average if for a free trace-preserving operation  $\Lambda$  and its representation in terms of free Kraus operators  $\{K_{\lambda}\}$

$$\mathcal{M}(\rho) \geq \int d\lambda p(\lambda|\rho) \mathcal{M}(\sigma_{\lambda}), \quad (4)$$

$$\text{for } \Lambda(\rho) = \int d\lambda p(\lambda|\rho) \sigma_{\lambda} \quad \text{and} \quad \sigma_{\lambda} = \frac{1}{p(\lambda|\rho)} K_{\lambda} \rho K_{\lambda}^{\dagger}.$$

For practical purposes, it is useful to consider a finite discrete set of Kraus operators, which leads to the following property, using the same notations as in the previous definition:

**Definition 5** (Monotonicity on average (operational)). A monotone  $\mathcal{M}$  is called monotone on average in the operational sense if

$$\mathcal{M}(\rho) \geq \sum_i p_{i|\rho} \mathcal{M}(\sigma_i), \quad (5)$$

$$\text{for } \Lambda(\rho) = \sum_i p_{i|\rho} \sigma_i \quad \text{and} \quad \sigma_i = \frac{1}{p_{i|\rho}} K_i \rho K_i^{\dagger}.$$

Monotonicity on average allows for investigating probabilistic operations. This is an important property especially when one is considering quantum optics, where genuine non-Gaussianity is usually generated in a probabilistic fashion. A monotone having the property of monotonicity on average allows for computing bounds including probabilistic protocols. Indeed, given a resource monotone  $\mathcal{M}$ , if  $\Lambda$  is a free operation that maps  $k$  copies of  $\rho$  to  $m$  copies of  $\sigma$  with probability  $p$ , then monotonicity on average implies [1]:

$$\mathcal{M}(\rho^{\otimes k}) \geq p \mathcal{M}(\sigma^{\otimes m}). \quad (6)$$

## 2.2 Continuous-variable quantum information

In this section we provide a brief review of CV quantum information theory, with particular emphasis on Gaussian quantum information in section 2.2.1 and the stellar representation of non-Gaussian states in section 2.2.2. We refer the reader to [24, 25, 30] for more in-depth treatments.

### 2.2.1 Gaussian quantum information theory

Gaussian quantum optics offers a rich area of research, where a vast set of tools and analytical techniques are available [13, 30]. In this work we denote the creation and annihilation operators by  $\hat{a}, \hat{a}^{\dagger}$ , which satisfy the canonical commutation relation

$$[\hat{a}, \hat{a}^{\dagger}] = \hat{1}. \quad (7)$$

We denote by  $\hat{\mathbf{a}} = (\hat{a}_1, \dots, \hat{a}_m)^T$  the tuple of annihilation operators over  $m$  modes. Gaussian unitaries are defined as

$$\hat{U}_G = e^{-i\hat{H}_G}, \quad (8)$$

where  $\hat{H}_G$  is at most quadratic in the creation and annihilation operators of the modes:

$$\hat{H}_G = \boldsymbol{\alpha}^T \hat{\mathbf{a}}^{\dagger} + \hat{\mathbf{a}}^{\dagger} U \hat{\mathbf{a}} + \hat{\mathbf{a}}^{\dagger} S \hat{\mathbf{a}}^{\dagger} + H.c., \quad (9)$$

for  $\boldsymbol{\alpha} \in \mathbb{C}^m$  and where  $U, S$  are  $m \times m$  complex matrices for  $m$  modes. Gaussian unitary operators map creation and annihilation operators into affine symplectic combinations of creation and annihilation operators.

A generic single-mode Gaussian unitary can be decomposed into a sequence of displacements,

squeezing and phase shifts:

$$\hat{D}(\alpha) = e^{\alpha \hat{a}^\dagger - \alpha^* \hat{a}}, \quad (10)$$

$$\hat{S}(\xi) = e^{\frac{1}{2}(\xi \hat{a}^{\dagger 2} - \xi^* \hat{a}^2)}, \quad (11)$$

$$\hat{R}(\phi) = e^{i\phi \hat{a}^\dagger \hat{a}}. \quad (12)$$

To decompose multimode Gaussian unitaries, an additional non-trivial 2-mode unitary is sufficient. For example, one can consider the operation associated to the action of a beam splitter:

$$\hat{U}_{BS}(\theta) = e^{\theta(\hat{a}_1^\dagger \hat{a}_2 - \hat{a}_1 \hat{a}_2^\dagger)}, \quad (13)$$

where the variable  $\theta$  sets the transmissivity of the beamsplitter  $\tau = \cos(\theta)^2$  — which is called balanced if  $\tau = \frac{1}{2}$  or equivalently  $\theta = \frac{\pi}{4}$ .

More generally one can define the passive Gaussian operations as those that conserve the total number of photons. These unitary operators are generated by Hamiltonians of the form  $\hat{H}_p = \hat{a}^\dagger U \hat{a} + H.c.$ . Any (multimode) Gaussian unitary can, as a consequence of the Euler (sometimes called Bloch–Messiah) decomposition, be decomposed as

$$\hat{U}_G = \hat{U} \hat{S}(\xi) \hat{D}(\alpha) \hat{V}, \quad (14)$$

where  $\hat{U}$  and  $\hat{V}$  are passive Gaussian unitary operators.

A general Gaussian state is defined as

$$\rho_G = \frac{e^{-\beta \hat{H}_G}}{\text{Tr}[e^{-\beta \hat{H}_G}]} \quad (15)$$

including the case  $\beta \rightarrow \infty$  for pure states. For pure states, this is equivalent to

$$|\psi_G\rangle = \hat{U}_G |\mathbf{0}\rangle \quad (16)$$

$$= \hat{U} \hat{S}(\xi) \hat{D}(\alpha) |\mathbf{0}\rangle, \quad (17)$$

where  $|\mathbf{0}\rangle$  denotes the tensor product of  $m$  vacua and where we used the fact that passive Gaussian unitary operators map the vacuum state to itself in the last line.

We define Gaussian protocols as follows [22]:

**Definition 6.** A Gaussian protocol is a map from  $\rho \in \mathcal{H}$  to  $\sigma \in \mathcal{H}'$  composed of the following operations

- Gaussian unitaries:  $\rho \mapsto \hat{U}_G \rho \hat{U}_G^\dagger$
- Composition with pure Gaussian state:  $\rho \mapsto \rho \otimes |\psi_G\rangle\langle\psi_G|$ .

- Pure Gaussian measurement of subsystem:  $\rho \mapsto \text{Tr}_S[\rho(\mathbf{1} \otimes |\psi_G(\alpha)\rangle\langle\psi_G(\alpha)|)]/p(\alpha|\rho)$ , where  $p(\alpha|\rho) = \text{Tr}[\rho(\mathbf{1} \otimes |\psi_G(\alpha)\rangle\langle\psi_G(\alpha)|)]$  and  $\alpha$  is a vector of real measurement outcomes.

- Partial trace on subsystems:  $\rho \mapsto \text{Tr}_S[\rho]$ .
- The above operations conditioned on classical randomness or
  - single measurement outcomes (ideal case);
  - measurement outcomes falling into finite-size intervals (operational case).

Despite the richness of Gaussian quantum optics, we cannot represent all possible states and operations using the Gaussian manifold. More critically, when restricting to Gaussian protocols acting on Gaussian states, achieving exponential quantum computational advantage becomes impossible, as such processes can be efficiently simulated using classical algorithms [30]. The setting of Gaussian quantum information processing is moreover limited by several no-go results for various tasks, including entanglement distillation [31–33], error correction [34], and violation of Bell inequalities/contextuality [35]. Thus, in order to obtain genuine quantum phenomena beyond what is classical simulatable, we need to include non-Gaussian operations or states.

## 2.2.2 The stellar representation of non-Gaussian states

The stellar representation has been introduced in [24] to characterize single-mode non-Gaussian quantum states and is related to the notion of genuine  $n$ -photon non-Gaussianity [26]. It has later been generalised to the multimode setting in [25, 36, 37]. In this section, we give a brief review of this formalism.

The stellar representation classifies CV quantum states using the so-called *stellar function* (or Bargmann, Fock–Bargmann, Segal–Bargmann function), which is a representation of a quantum state in an infinite-dimensional Hilbert space by a holomorphic function originally due to Segal [38] and Bargmann [39]. More precisely, to any  $m$ -mode pure quantum state  $|\psi\rangle = \sum_{\mathbf{n} \geq \mathbf{0}} \psi_{\mathbf{n}} |\mathbf{n}\rangle$  is

associated its stellar function

$$F_{\psi}^*(z) := \sum_{n \geq 0} \frac{\psi_n}{\sqrt{n!}} z^n, \quad (18)$$

for all  $z \in \mathbb{C}^m$ .

The algebraic structure of this function allows us to rank CV quantum states using the *stellar rank*: pure quantum states of finite stellar rank  $r^* \in \mathbb{N}$  are those states whose stellar function is of the form  $P \times G$ , where  $P$  is a multivariate polynomial of degree  $r^*$  and  $G$  is a multivariate Gaussian function, while the other states are of infinite stellar rank. For a mixed state  $\rho$ , the stellar rank is defined using a convex roof construction:  $r^*(\rho) = \inf_{p_i, \psi_i} \sup r_{\psi_i}^*$ , where the infimum is over the decompositions  $\rho = \sum_i p_i |\psi_i\rangle\langle\psi_i|$ .

The stellar rank possesses remarkable properties—below we recall the ones which are used hereafter.

A unitary operation is Gaussian if and only if it leaves the stellar rank invariant, and the stellar rank is non-increasing under Gaussian channels and measurements [25]. As a result, the stellar rank is a non-Gaussian monotone which provides a measure of the non-Gaussian character of a quantum state and induces a non-Gaussian hierarchy among quantum states, the *stellar hierarchy* (see Fig. 1). At rank 0 of the hierarchy lie mixtures of Gaussian states, while quantum non-Gaussian states [40] populate all higher ranks. For instance, a multimode Fock state  $|n\rangle$  has stellar rank  $|n|$  [25], while a single-mode cat state has infinite stellar rank [24].

The stellar hierarchy bears an operational significance, because the stellar function gives a prescription for engineering a pure quantum state from the vacuum:  $|\psi\rangle = F_{\psi}^*(\hat{a}_1^\dagger, \dots, \hat{a}_m^\dagger) |0\rangle$ . As a result, a state of stellar rank  $n$  cannot be obtained from the vacuum by using less than  $n$  applications of creation operators, together with Gaussian unitary operations. In other words, the stellar rank has an operational interpretation as a lower bound on the minimal number of elementary non-Gaussian operations (applications of a single-mode creation operator, i.e. single-photon addition) needed to engineer the state from the vacuum.

The stellar hierarchy is robust with respect to the trace distance, i.e. every state of a given finite stellar rank only has states of equal or higher rank in a close vicinity [24, 25]. Moreover, states of finite stellar rank form a dense subset of the Hilbert

space, so that states of infinite rank can be approximated arbitrarily well in trace distance by sequences of states of finite stellar rank. The optimal approximation for any fixed rank can be obtained by an optimization over  $\mathcal{O}(m^2)$  parameters for  $m$ -mode states, independently of the rank. As a consequence, the stellar rank of quantum states can be witnessed experimentally [41, 42]. We elaborate on this property in section 3.3.

Finally, CV quantum computations with low stellar rank can be simulated efficiently using a classical computer [36, 43], which implies that the stellar rank is a necessary non-Gaussian resource for quantum computational speedup with CV.

Although it is a non-Gaussian monotone with valuable operational properties, the stellar rank is too crude of a measure when assessing Gaussian conversion protocols beyond exact conversion. Indeed, states of high stellar rank may be very close to states of much lower stellar rank, as can be illustrated by the states of the form  $|\psi_{\epsilon, N}\rangle = \sqrt{1-\epsilon}|0\rangle + \sqrt{\epsilon}|N\rangle$  for small  $\epsilon$  and large  $N$ . These are states of arbitrarily high stellar rank  $N$ , but up to a small perturbation  $\epsilon$  they are effectively of stellar rank 0.

In what follows, we introduce a fine-grained measure based on the stellar rank that allows us to assess Gaussian conversion protocols in practical situations, i.e., in both the exact and approximate cases.

### 3 The approximate stellar rank

#### 3.1 Definition

In the context of CV quantum information processing, identifying the minimal number of non-Gaussian operations required to engineer a desired quantum state up to a given precision is of paramount importance, especially for quantum optics platforms where such operations are hard to implement in a deterministic fashion. For this purpose, we introduce a new measure based on the stellar rank:

**Definition 7** (Approximate stellar rank). *For  $0 \leq \epsilon \leq 1$ , the  $\epsilon$ -approximate stellar rank of an  $m$ -mode density operator  $\rho$  is defined as*

$$r_{\epsilon}^*(\rho) := \inf_{\tau, F(\rho, \tau) \geq 1-\epsilon} r^*(\tau), \quad (19)$$

where  $F(\rho, \tau) = \text{Tr}(\sqrt{\sqrt{\rho}\tau\sqrt{\rho}})^2$  denotes the fidelity.

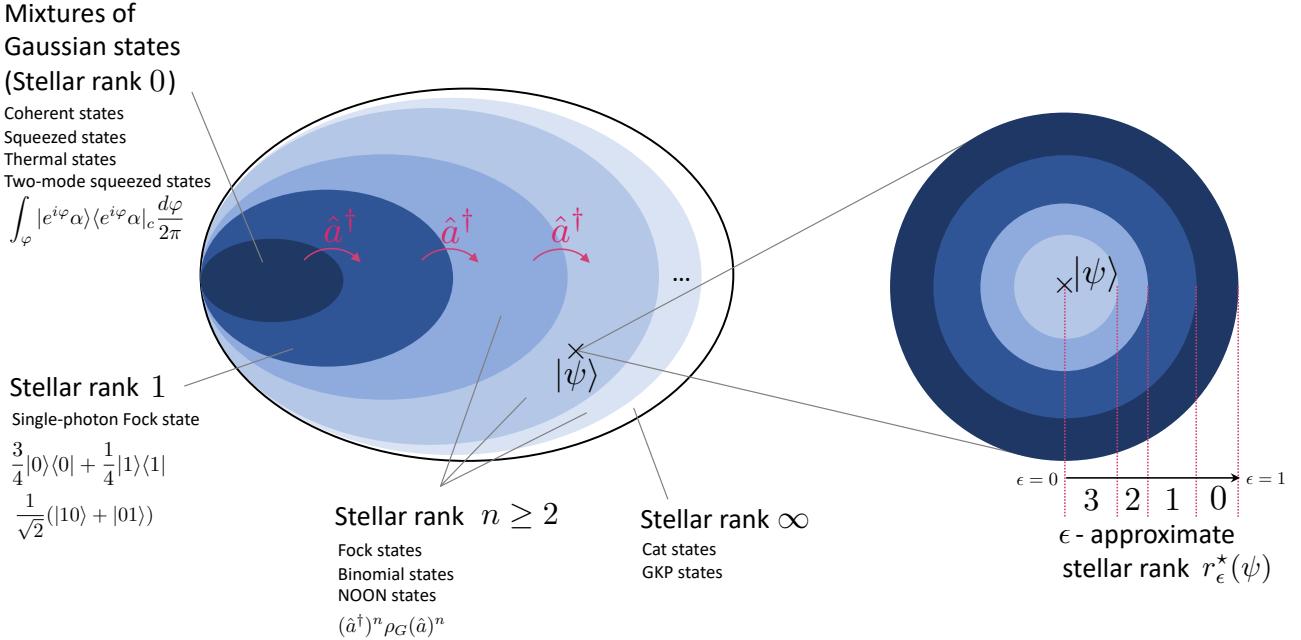


Figure 1: The set of quantum states, partitioned following the multimode stellar hierarchy (extended from [25]). For each rank, we give examples of states that are commonly encountered in the literature. The last example of stellar rank 0 is a rotation-invariant mixture of coherent states. The density matrix  $\rho_G$  denotes a Gaussian state. Gaussian unitary operators leave the stellar rank invariant, while non-Gaussian operators can increase it (such as the creation operator, which increases the stellar rank by one). The right hand side is a schematic representation of the topology of the hierarchy, at the vicinity of a pure state  $|\psi\rangle$  of stellar rank 3, illustrating how the  $\epsilon$ -approximate stellar rank decreases the further away one gets from  $|\psi\rangle$ .

The  $\epsilon$ -approximate stellar rank  $r_\epsilon^*$  is a generalisation of the stellar rank parametrised by  $\epsilon \in [0, 1]$ , with  $r_0^*(\rho) = r^*(\rho)$ . The infimum in the definition is defined with respect to the topology induced by the trace norm, and is actually a minimum, as the  $\epsilon$ -approximate stellar rank is an integer-valued, non-increasing function of  $\epsilon$ , with  $r_1^*(\rho) = 0$ . It gives the minimal stellar rank of states that are  $\epsilon$ -close in fidelity to a given state. From a mathematical standpoint, it quantifies how well a stellar function may be approximated by a function that is the product of a polynomial and a Gaussian, for increasing degree of the polynomial. Given the operational properties of the stellar rank, the  $\epsilon$ -approximate stellar rank can thus be understood as a minimal cost in terms of non-Gaussian operations to prepare an approximation of a target state.

A similar quantity known as the  $\epsilon$ -smoothed non-Gaussianity of formation has been previously introduced in the single-mode setting [24] and is readily generalised to the multimode setting:  $\mathcal{NGF}_\epsilon(\rho) := \min_{\tau, D(\rho, \tau) \leq \epsilon} r^*(\tau)$ , where

$D$  denotes the trace distance. By the Fuchs–van de Graaf inequalities, it satisfies  $r_\epsilon^*(\psi) \leq \mathcal{NGF}_\epsilon(\psi) \leq r_{\epsilon^2}^*(\psi)$  for pure states and  $r_{2\epsilon}^*(\rho) \leq \mathcal{NGF}_\epsilon(\rho) \leq r_{\epsilon^2}^*(\rho)$  in general, so these two quantities are operationally equivalent. Compared to the  $\epsilon$ -approximate stellar rank, the  $\epsilon$ -smoothed non-Gaussianity of formation measures the quality of the approximation using trace distance rather than fidelity. As a result, the  $\epsilon$ -smoothed non-Gaussianity of formation is challenging to compute, while the  $\epsilon$ -approximate stellar rank can be computed efficiently in several practical scenarios, as we show in section 3.3.

### 3.2 Properties

The stellar rank is sub-additive. Let  $\rho$  and  $\sigma$  be two density operators, then

$$\max[r^*(\rho), r^*(\sigma)] \leq r^*(\rho \otimes \sigma) \leq r^*(\rho) + r^*(\sigma). \quad (20)$$

In particular, it is additive if one of the density operators is a pure state or a mixture of Gaussian states [25].

On the other hand, for the  $\epsilon$ -approximate stellar rank, there are cases where  $r_\epsilon^*(\rho \otimes \sigma) > r_\epsilon^*(\rho) + r_\epsilon^*(\sigma)$ , even for pure states. For instance, consider the Fock state  $|1\rangle$ : writing  $f := 3\sqrt{3}/(4e) \approx 0.48$ , we have  $r_\epsilon^*(|1\rangle) = 1$  for  $0 \leq \epsilon < 1 - f$  and  $r_\epsilon^*(|1\rangle) = 0$  for  $1 - f \leq \epsilon \leq 1$  [24, 40], while  $r_\epsilon^*(|1\rangle^{\otimes 2}) = 2$  for  $0 \leq \epsilon < 1 - f$ ,  $r_\epsilon^*(|1\rangle^{\otimes 2}) = 1$  for  $1 - f \leq \epsilon < 3/4$ , and  $r_\epsilon^*(|1\rangle^{\otimes 2}) = 0$  for  $3/4 \leq \epsilon \leq 1$  [41]<sup>1</sup>. In particular, the  $\epsilon$ -approximate stellar rank of the Fock state  $|1\rangle$  satisfies  $1 = r_\epsilon^*(|1\rangle^{\otimes 2}) > 2r_\epsilon^*(|1\rangle) = 0$  for  $1 - f \leq \epsilon < 3/4$ . This means that for a fixed  $\epsilon$ , the  $\epsilon$ -approximate stellar rank is generally not sub-additive. However, by allowing for different values of  $\epsilon$ , we show that the approximate stellar rank does satisfy a sub-additivity property for pure states:

**Lemma 1** (Sub-additivity of the approximate stellar rank). *Let  $k \geq 1$  and let  $|\psi_1\rangle, \dots, |\psi_k\rangle$  be pure states. Let  $\epsilon = (\epsilon_1, \dots, \epsilon_k) \in [0, 1]^k$  with  $|\epsilon| = \epsilon_1 + \dots + \epsilon_k \leq 1$ . Then*

$$\max_{i=1 \dots k} r_{|\epsilon|}^*(\psi_i) \leq r_{|\epsilon|}^*\left(\bigotimes_{i=1}^k \psi_i\right) \leq \sum_{i=1}^k r_{\epsilon_i}^*(\psi_i). \quad (21)$$

In particular, setting  $|\psi_1\rangle = \dots = |\psi_k\rangle = |\psi\rangle$  and  $\epsilon_1 = \dots = \epsilon_k = \frac{\epsilon}{k}$  gives

$$r_\epsilon^*(\psi) \leq r_\epsilon^*(\psi^{\otimes k}) \leq k r_{\epsilon/k}^*(\psi). \quad (22)$$

We give a proof in Appendix A.

The relevance of the  $\epsilon$ -approximate stellar rank for Gaussian conversion comes from the following result:

**Theorem 1** (The approximate stellar rank is a monotone). *For all  $0 \leq \epsilon \leq 1$ , the  $\epsilon$ -approximate stellar rank is a non-Gaussian monotone which vanishes for Gaussian states and is also monotone on average (ideal and operational).*

We give a proof in Appendix A. This result has direct consequences for Gaussian conversion, which we detail in section 4.

### 3.3 Computation

The  $\epsilon$ -approximate stellar rank is closely related to the notion of maximum achievable fidelity using states of bounded stellar rank introduced in [41], or *stellar fidelities* for short:

<sup>1</sup>Note that these are corrected versions of the numerical values originally given in that paper.

**Definition 8** (Stellar fidelities). *The stellar fidelities of a state  $\rho$  are defined as*

$$f_n^*(\rho) := \sup_{\tau, r^*(\tau) \leq n} F(\rho, \tau), \quad (23)$$

for all  $n \in \mathbb{N}$ .

We have  $f_n^*(\rho) = 1$  for all  $n \geq r^*(\rho)$ . The supremum in the definition is defined with respect to the topology induced by the trace norm, and is actually a maximum, as the sets of states of stellar rank bounded by  $n \in \mathbb{N}$  are closed [24, 25] and  $\tau \mapsto F(\rho, \tau)$  is continuous (see Lemma 5).

From Definitions 7 and 8, we obtain the following relation between approximate stellar rank and stellar fidelities:

**Lemma 2** (Equivalence between approximate stellar rank and stellar fidelities). *For all  $n \in \mathbb{N}$  and all  $0 \leq \epsilon \leq 1$ ,*

$$r_\epsilon^*(\rho) \leq n \Leftrightarrow 1 - \epsilon \leq f_n^*(\rho), \quad (24)$$

or equivalently, for all  $1 \leq n < r^*(\rho)$ ,

$$r_\epsilon^*(\rho) = \begin{cases} r^*(\rho) & \text{for } \epsilon \in [0, 1 - f_{r^*(\rho)-1}^*(\rho)), \\ n & \text{for } \epsilon \in [1 - f_n^*(\rho), 1 - f_{n-1}^*(\rho)), \\ 0 & \text{for } \epsilon \in [1 - f_0^*(\rho), 1]. \end{cases} \quad (25)$$

This implies that the values of the stellar fidelities  $f_n^*(\rho)$  for all  $n$  specify the values of the  $\epsilon$ -approximate stellar rank  $r_\epsilon^*(\rho)$  for all  $0 \leq \epsilon \leq 1$ , and vice versa, as illustrated in Fig. 2.

As it turns out, computing the stellar fidelities of pure states over a few modes is efficient, because it can be reduced to an optimisation over a subset of Gaussian unitaries. Let us write, for all  $n \in \mathbb{N}$ ,

$$\Pi_n = \sum_{|\mathbf{p}| \leq n} |\mathbf{p}\rangle\langle\mathbf{p}|, \quad (26)$$

the projector onto the subspace of  $m$ -mode states with at most  $n$  photons. From Theorem 2 in [41]:

**Theorem 2** (Computation of stellar fidelities [41]). *Let  $n \in \mathbb{N}$  and let  $|\psi\rangle$  be a  $m$ -mode target pure state. Then, the maximum achievable fidelity with the target state  $|\psi\rangle$  using  $m$ -mode states of finite stellar rank less or equal to  $n$  is given by*

$$f_n^*(\psi) = \max_{\hat{G}} \langle \psi | \hat{G}^\dagger \Pi_n \hat{G} | \psi \rangle, \quad (27)$$

where the supremum is over  $m$ -mode Gaussian unitary operations of the form  $\hat{G} = \hat{S}\hat{D}\hat{U}$ , where  $\hat{S}$  is a tensor product of squeezing operators with real-valued squeezing parameters,  $\hat{D}$  is a tensor product of displacement operators and  $\hat{U}$  is a passive linear operator. Moreover, assuming the optimisation yields a Gaussian operation  $\hat{G}_0$ , an optimal approximating state of stellar rank at most  $n$  is  $\hat{G}_0^\dagger \Pi_n \hat{G}_0 |\psi\rangle$ , up to normalisation.

In particular, given a target state  $|\psi\rangle$ , this result allows us to compute the set of achievable fidelities with that state using states of finite stellar rank  $n$  for all  $n \in \mathbb{N}$ , i.e., the profile of stellar fidelities of  $|\psi\rangle$ . The values of the  $\epsilon$ -approximate stellar rank for all  $\epsilon$  can then be read from this profile, via Lemma 2 (see Fig. 2).

A limitation of this technique is that the numerical bounds derived do not come with a certificate: the  $\epsilon$ -approximate stellar rank is obtained by a minimization over a non-convex space, so we cannot be sure in general that the numerical value obtained corresponds to the global optimum. For many practical examples, however, the optimisation space is small enough so that we can have high confidence about the numerical bounds obtained. This is the case in particular for most single-mode examples, which lead to trustful bounds for multimode cases as well using the sub-additivity bounds from Lemma 1, as we show in the next section. We provide a code for computing stellar fidelities of arbitrary single-mode superpositions of Fock states [here](#) [44].

## 4 Gaussian conversion

Gaussian conversion amounts to producing non-Gaussian states from other non-Gaussian states via Gaussian protocols (see Definition 6). It includes protocols such as non-Gaussian distillation or non-Gaussian state breeding, among others [23, 28, 29, 45–51].

Quantum state conversion can be exact or approximate, deterministic or probabilistic (heralded). In what follows, we study both deterministic and probabilistic cases under the same umbrella. We focus on exact Gaussian conversion in section 4.1 and on approximate Gaussian conversion in 4.2. Throughout this section, we use the Gaussian conversion from  $|2\rangle$  to  $|1\rangle \otimes |1\rangle$  as a guiding pedagogical example. We further

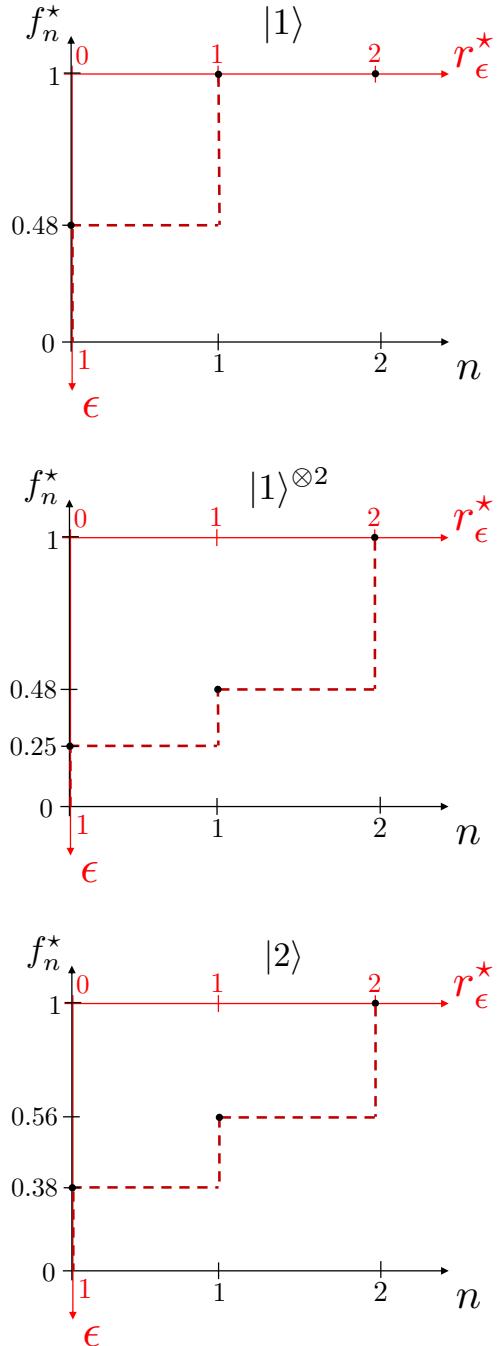


Figure 2: Stellar fidelities (in black) and approximate stellar rank (in red) of the Fock states  $|1\rangle$ ,  $|1\rangle^{\otimes 2}$  and  $|2\rangle$ , as a function of stellar rank  $n$  and approximation parameter  $\epsilon$ , respectively. In each profile, each black dot represents a stellar fidelity  $f_n^*$ , while each dashed line gives the  $\epsilon$ -approximate stellar rank.

illustrate our results with numerical examples inspired from Gaussian conversion protocols which have been studied theoretically and/or demonstrated experimentally in sections 4.3 and 5.

## 4.1 Exact Gaussian conversion bounds

In this section, we illustrate the use of approximate stellar rank for assessing exact Gaussian conversion. Note that exact conversion is a particular case of approximate conversion (when the error parameter is set to 0) which we analyse in the next section 4.2.

Recall from section 2.1 and Eq. (6) that any non-Gaussian monotone  $\mathcal{M}$  which is monotone on average yields

$$\mathcal{M}(\rho^{\otimes k}) \geq p \mathcal{M}(\sigma^{\otimes m}) \quad (28)$$

when exact Gaussian conversion of  $k$  copies of  $\rho$  to  $m$  copies of  $\sigma$  with probability  $p$  is possible.

The Wigner Logarithmic Negativity (WLN) is defined as  $W(\rho) = \log f|W_\rho|$ , where  $W_\rho$  is the Wigner function. It has been used as a non-Gaussian monotone to assess exact Gaussian conversion protocols in Ref. [22], both in deterministic and probabilistic cases. Since it is a non-Gaussian monotone [25], the stellar rank can also be used to assess exact Gaussian conversion protocols, in a way that is somewhat complementary to negativity of the Wigner function. For instance, a cat state and a Fock state  $|1\rangle$  can have the same Wigner negativity for a well-chosen cat state amplitude, but the former has infinite stellar rank while the latter has finite stellar rank (equal to 1), so exact Gaussian conversion from the Fock state to the cat is impossible, which Wigner negativity cannot conclude. However, quantum states with the same stellar rank can have different Wigner negativity. For instance, the Wigner negativity of the state  $|1\rangle \otimes |1\rangle$  is about 0.71, while that of the state  $|2\rangle$  is about 0.55 [21], even though both states have stellar rank 2. Moreover, unlike stellar rank, Wigner negativity is robust to small perturbations: consider the example pointed out earlier of the states  $|1\rangle$  and  $|\psi_{\epsilon,1}\rangle = \sqrt{1-\epsilon}|0\rangle + \sqrt{\epsilon}|1\rangle$ . Both states have stellar rank 1, but Wigner negativity clearly tells us that conversion from the latter state to the former is impossible for small  $\epsilon$ .

Hereafter, we show that the  $\epsilon$ -approximate stellar rank provides the best of both worlds when assessing exact Gaussian conversion:

**Lemma 3** (Exact conversion bounds with approximate stellar rank). *If  $m$  copies of  $\sigma$  can be obtained from  $k$  copies of  $\rho$  with probability  $p$  us-*

*ing Gaussian operations, then for all  $0 \leq \epsilon \leq 1$ :*

$$r_\epsilon^*(\rho^{\otimes k}) \geq p r_\epsilon^*(\sigma^{\otimes m}). \quad (29)$$

This Lemma is a direct consequence of Eq. (28) and Theorem 1.

By Lemma 2, for deterministic conversion  $p = 1$ , this continuum of conditions is equivalent a discrete set of conditions, namely that for each stellar rank the maximum achievable fidelity with  $\rho^{\otimes k}$  is smaller than the maximum achievable fidelity with  $\sigma^{\otimes m}$ . From a graphical perspective, this means that the profile of stellar fidelities of the input is below that of the output. This is easily generalised to probabilistic conversion:

**Lemma 4** (Exact conversion bounds with stellar fidelities). *If  $m$  copies of  $\sigma$  can be obtained from  $k$  copies of  $\rho$  with probability  $p$  using Gaussian operations, then for all  $n \in \mathbb{N}$ :*

$$f_n^*(\rho^{\otimes k}) \leq f_{[n/p]}^*(\sigma^{\otimes m}). \quad (30)$$

We give a quick proof in Appendix B, which combines Lemmas 2 and 3. From a graphical perspective, this means that the profile of stellar fidelities of the input is below that of the output, after the latter has been horizontally scaled up by a factor  $1/p$ .

Let us illustrate the use of these bounds for the Gaussian conversion  $|2\rangle \mapsto |1\rangle \otimes |1\rangle$ . As we have mentioned previously, in this case, the WLN for these two states is easily computed numerically as  $W(|2\rangle) \simeq 0.55$  and  $W(|1\rangle^{\otimes 2}) = 0.71$ . Since WLN is monotone on average [22], Eq. (28) yields  $W(|2\rangle) \geq p W(|1\rangle^{\otimes 2})$  when exact Gaussian conversion is potentially possible with probability  $p$ , which implies that exact Gaussian conversion from  $|2\rangle$  to  $|1\rangle^{\otimes 2}$  with probability  $p$  is impossible whenever  $p > 0.55/0.71 \simeq 0.77$ . Now the first stellar fidelities for these states are given by Theorem 2 as  $f_0^*(|2\rangle) \simeq 0.38$  and  $f_0^*(|1\rangle^{\otimes 2}) \simeq 0.25$ , so with  $n = 0$ , Lemma 4 implies that exact Gaussian conversion from  $|2\rangle$  to  $|1\rangle^{\otimes 2}$  is actually impossible for any probability  $p$ .

As this example illustrates, the bound  $f_0^*(\rho^{\otimes k}) \leq f_0^*(\sigma^{\otimes m})$  based on stellar fidelity for  $n = 0$  is independent of the probability of success  $p$  of the Gaussian conversion. As such, it constitutes a powerful tool to rule out exact Gaussian conversion, leading to a large family of no-goes beyond state-of-the-art, as we show in section 4.3. We also generalise it to approximate Gaussian conversion in the next section.

Note that for a pure state  $\psi$ , this stellar fidelity  $f_0^*(\psi)$  is the maximal fidelity with a pure Gaussian state. Note here the connection with the Gaussian extent [27] that is an alternative non-Gaussian measure. For some classes of states, such as for example Fock states, the Gaussian extent is the inverse of the maximal fidelity with a pure Gaussian state [27, 52].

For the simple example  $|2\rangle \mapsto |1\rangle \otimes |1\rangle$ , the approximate stellar rank (or equivalently, the stellar fidelities) is more informative than Wigner negativity, which is also currently limited to the case of exact Gaussian conversion. In the following section, we extend all our bounds to the case of approximate Gaussian conversion.

## 4.2 Approximate Gaussian conversion bounds

The bounds derived in the previous section can be extended to the more general case of approximate Gaussian conversion, in which the output state of the conversion protocol is only guaranteed to be  $\delta$ -close in trace distance to the target state, for some error parameter  $\delta \geq 0$ :

**Theorem 3** (Approximate conversion bounds with approximate stellar rank). *If a state  $\delta$ -close in trace distance to  $m$  copies of  $\sigma$  can be obtained from  $k$  copies of  $\rho$  with probability  $p$  using Gaussian operations, then for all  $0 \leq \epsilon \leq 1 - \delta$*

$$r_\epsilon^*(\rho^{\otimes k}) \geq p r_{\epsilon+\sqrt{2\delta}}^*(\sigma^{\otimes m}). \quad (31)$$

Moreover, if  $\rho = \psi$  and  $\sigma = \phi$  are pure states,

$$r_\epsilon^*(\psi^{\otimes k}) \geq p r_{\epsilon+\delta}^*(\phi^{\otimes m}). \quad (32)$$

We give a proof in Appendix C.

As in the previous section, by Lemma 2, for deterministic conversion  $p = 1$ , this continuum of conditions is equivalent a discrete set of conditions, namely that for each stellar rank the maximum achievable fidelity with  $\rho^{\otimes k}$  is greater than the maximum achievable fidelity with  $\sigma^{\otimes m}$  by at most an amount  $\sqrt{2\delta}$  ( $\delta$  for pure states). From a graphical perspective, this means that the profile of stellar fidelities of the input is below that of the output, after lowering the former by vertical offset depending on  $\delta$ . This is easily generalised to probabilistic conversion, with a similar proof to Lemma 4:

**Theorem 4** (Approximate conversion bounds with stellar fidelities). *If a state  $\delta$ -close in trace*

*distance to  $m$  copies of  $\sigma$  can be obtained from  $k$  copies of  $\rho$  with probability  $p$  using Gaussian operations, then for all  $n \in \mathbb{N}$ :*

$$f_n^*(\rho^{\otimes k}) \leq f_{\lfloor n/p \rfloor}^*(\sigma^{\otimes m}) + \sqrt{2\delta}. \quad (33)$$

Moreover, if  $\rho = \psi$  and  $\sigma = \phi$  are pure states,

$$f_n^*(\psi^{\otimes k}) \leq f_{\lfloor n/p \rfloor}^*(\phi^{\otimes m}) + \delta. \quad (34)$$

Any  $n$  such that the bound in Theorem 4 is violated rules out approximate Gaussian conversion from  $\rho^{\otimes k}$  to  $\sigma^{\otimes m}$  with probability greater than  $p$  and trace distance error smaller than  $\delta$ . Note that, similar to the case of exact Gaussian conversion, the bounds corresponding to  $n = 0$  are independent of  $p$ :

$$f_0^*(\rho^{\otimes k}) \leq f_0^*(\sigma^{\otimes m}) + \sqrt{2\delta} \quad (35)$$

$$f_0^*(\psi^{\otimes k}) \leq f_0^*(\phi^{\otimes m}) + \delta. \quad (36)$$

This implies that a violation of the bound (35) (resp. (36)) witnesses impossibility of approximate Gaussian conversion from  $|\rho\rangle^{\otimes k}$  to  $|\sigma\rangle^{\otimes m}$  (resp. from  $|\psi\rangle^{\otimes k}$  to  $|\phi\rangle^{\otimes m}$ ) with trace distance error smaller than  $\delta$ , for any probability of success  $p$ .

Using Theorem 2, we can compute the stellar fidelities for pure states over few modes efficiently. For many copies, however, the stellar fidelities may be challenging to compute. To tackle this issue, we restrict the output to be a single copy ( $m = 1$ ), which is the case of interest in most resource conversion protocols, and we use Lemma 1 which gives bounds depending only on single-copy quantities to recover the case of pure states over few modes:

**Theorem 5** (Approximate conversion bounds based on single-copy quantities). *If a state  $\delta$ -close in trace distance to a single copy of  $\phi$  can be obtained from  $k$  copies of  $\psi$  with probability  $p$  using Gaussian operations, then for all  $0 \leq \epsilon \leq 1 - \delta$ ,*

$$k r_{\epsilon/k}^*(\psi) \geq p r_{\epsilon+\delta}^*(\phi). \quad (37)$$

or equivalently with Lemma 2:

$$1 - f_{\lfloor \frac{kn}{p} \rfloor}^*(\phi) \leq k(1 - f_n^*(\psi)) + \delta, \quad (38)$$

for all  $n \in \mathbb{N}$ .

### 4.3 No-go regions for Gaussian conversion

The bounds in Theorems 4 and 5 imply the existence of *no-go (or excluded) regions* for Gaussian conversion, i.e., values of the success probability  $p$  and the trace distance error  $\delta$  such that Gaussian conversion is impossible, because one of the Gaussian conversion bounds is being violated.

Notice by Eq. (37) that for  $n > 0$ , the only values of  $p$  that need to be checked are such that  $\frac{kn}{p}$  is an integer, i.e.,  $p = \frac{kn}{q}$ , for  $q = kn, \dots, r^*(\phi)$ . As a consequence, the no-go region given by Theorem 4 for the Gaussian conversion  $|\psi\rangle^{\otimes k} \mapsto |\phi\rangle^{\otimes m}$  with success probability  $p$  and trace distance error  $\delta$  is the union of the rectangles:

$$(p, \delta) \in \left(\frac{n}{q}, 1\right] \times [0, f_n^*(\psi^{\otimes k}) - f_q^*(\phi^{\otimes m})], \quad (39)$$

for  $n = 1, \dots, r^*(\psi^{\otimes k})$  and  $q = n, \dots, r^*(\phi^{\otimes m})$ , together with the rectangle:

$$(p, \delta) \in (0, 1] \times [0, f_0^*(\psi^{\otimes k}) - f_0^*(\phi^{\otimes m})], \quad (40)$$

for  $n = 0$ . The boundary of the no-go region  $(p, \delta)$  is a non-decreasing step function, as ruling out the possibility of Gaussian conversion for a specific value of  $(p, \delta)$  also rules it out for higher success probability and smaller approximation error. We show the corresponding no-go region for the example of the Gaussian conversion  $|2\rangle \mapsto |1\rangle \otimes |1\rangle$  in Fig. 3. We see that independent of the success probability there is always a non-zero error, i.e., we cannot get closer in trace distance than what is indicated by the blue region. Even more, the no-go region is one rectangle meaning that we cannot decrease the error by reducing the success probability; the error is independent of the success probability.

Similarly, the no-go region given by the sub-additivity bounds in Theorem 5 for Gaussian conversion  $|\psi\rangle^{\otimes k} \mapsto |\phi\rangle$  with success probability  $p$  and trace distance error  $\delta$  is the union of the rectangles:

$$(p, \delta) \in \left(\frac{kn}{q}, 1\right] \times \left[0, 1 - f_q^*(\phi) - k(1 - f_n^*(\psi))\right], \quad (41)$$

for  $n = 1, \dots, r^*(\psi)$  and  $q = kn, \dots, r^*(\phi)$ , together with the rectangle:

$$(p, \delta) \in (0, 1] \times \left[0, 1 - f_0^*(\phi) - k(1 - f_0^*(\psi))\right], \quad (42)$$

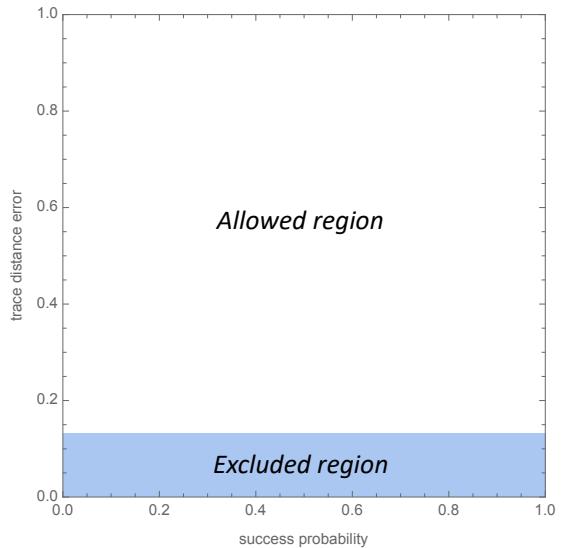


Figure 3: In blue: no-go region for (approximate, probabilistic) Gaussian conversion  $|2\rangle \mapsto |1\rangle \otimes |1\rangle$ . This region is given by the rectangle in Eq. (40) for  $|\psi\rangle = |2\rangle$ ,  $k = 1$ ,  $|\phi\rangle = |1\rangle$ ,  $m = 2$ , the other rectangles in Eq. (39) being included in that one.

for  $n = 0$ . These no-go regions, albeit less tight than the ones given by Theorem 4 (due to the use of sub-additive bounds) are already very informative.

These lead to several no-goes beyond state-of-the-art for Gaussian conversion between CV states. For instance, no-goes for Gaussian conversion have been obtained in [53] in the case of deterministic and exact conversion restricted to passive Gaussian operations (linear optics). Our results subsume several of these no-goes as they are generally valid for approximate and probabilistic Gaussian scenarios. We provide code for computing no-go regions for Gaussian conversion from stellar fidelities [here](#) [44]. We further provide illustrating examples of no-go regions in Figures 4 and 5, in the case of a target physical GKP state (with parameters  $\Delta = \frac{1}{\kappa} = 0.1$  [54]), and emphasize that our results are applicable to any choice of input states  $|\psi\rangle^{\otimes k}$  and output state  $|\phi\rangle$ .

As we see in Fig. 4, if only one Fock state  $|1\rangle$  is used then the error is lower bounded and we can never achieve a Gaussian conversion lower than this error independent of the success probability. For more copies a region opens where for small success probabilities an exact conversion cannot be ruled out. Increasing the number of copies further, this region widens and conversion with higher success probabilities cannot be ruled out.

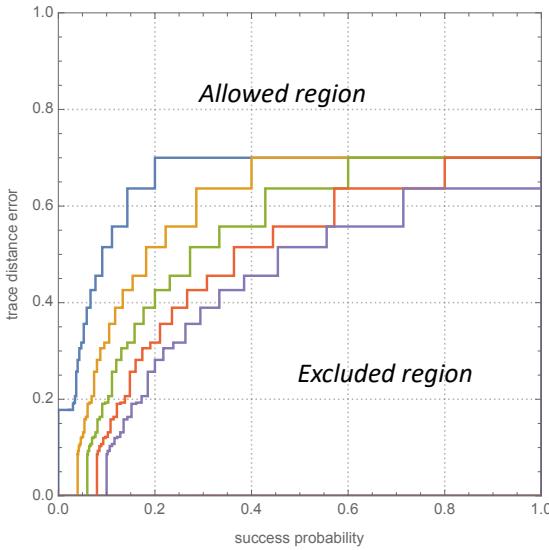


Figure 4: No-go regions for the Gaussian conversions of  $k$  copies of a single-photon Fock state  $|1\rangle^{\otimes k}$  to a single physical GKP state  $|\text{GKP}_\Delta\rangle$ . For clarity, only the boundaries are represented. The various regions correspond to a number of copies  $k$  from 1 (blue curve) to 5 (purple curve), with the size of the region decreasing as the number of copies increases. The target GKP state has  $\Delta = 0.1$ .

Furthermore, the error decreases overall with increasing the number of copies.

Instead of looking into multiple copies of Fock states, we can study different input states. In Fig. 5, we show the no-go region for a Gaussian conversion from an odd cat state to the same GKP state targeted before. Again we see here that all of these conversion have a lower bounded error; independently of the success probability one can never achieve Gaussian conversion below a certain error. By increasing the amplitude of the cat state, i.e., using more non-Gaussian resources, we can however make the excluded area smaller and less conversions are ruled out.

## 5 Assessing Gaussian conversion protocols

It is necessary to minimize the resources required to perform any quantum computational task or protocol. Resource monotones are an important tool to aid this problem by offering the possibility to obtain fundamental lower bounds on how many resources are required for a given task. If a

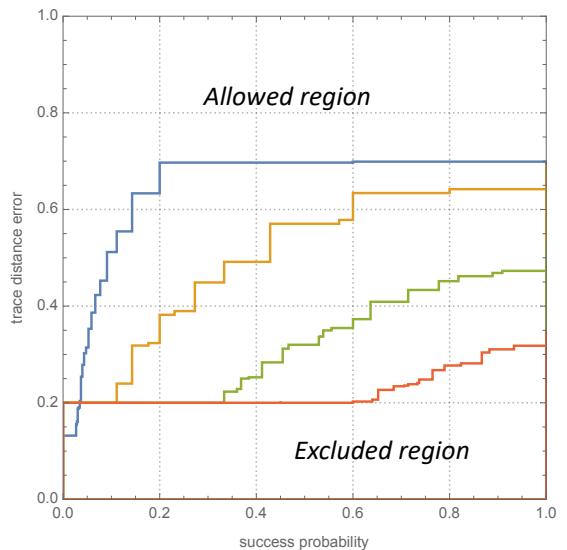


Figure 5: No-go regions for the Gaussian conversions of a single copy of an odd cat state  $\propto |\alpha\rangle - |-\alpha\rangle$  to a physical GKP state  $|\text{GKP}_\Delta\rangle$ . For clarity, only the boundaries are represented. The various regions correspond to a cat state amplitude  $\alpha = 1$  (blue), 3 (orange), 6 (green) and 10 (red), with the size of the region decreasing as the amplitude increases. The target GKP state has  $\Delta = 0.1$ .

protocol saturates these bounds, there is no hope on improving the protocol further. However, if there is a gap between a lower bound and the best existing protocol there is the possibility of improving the protocol to use the resource more efficiently and improve experimental practicality.

In this section, we provide a general methodology to harness our results on the approximate stellar rank in order to find lower bounds on Gaussian state conversion protocols, in the setting of both approximate and probabilistic conversions. We then illustrate this methodology on a specific protocol [28].

### 5.1 Methodology

In practice, we use Theorem 5 as our main tool for assessing Gaussian conversion protocols. To do so, we follow these steps:

1. Choose a (pure state, many-to-one) Gaussian conversion scenario, given by  $k$  copies of a pure input state  $|\psi\rangle$  and a target pure state  $|\phi\rangle$ .
2. Compute numerically the profiles of stellar

- fidelities for  $|\psi\rangle$  and  $|\phi\rangle$  using Theorem 2.
3. Compute the no-go regions for  $(p, \delta)$ , where  $p$  is the success probability and  $\delta$  the error to the target state in trace distance using Eqs. (41) and (42).
  4. Compare the success probability and approximation error of the Gaussian conversion protocol with the boundary of the no-go region.

We provide efficient code hosted on a public repository [44] to implement this procedure.

## 5.2 Numerical study

Notable Gaussian conversion protocols that were previously studied include: conversion of two single-photons into a two-photon state [22]; conversion of Fock states to cat states [45]; synthesis of GKP states from several non-Gaussian states [46–48, 55]; conversion of trisqueezed state to cubic phase state [28, 29];  $n$ -photon added or  $n$ -photon subtracted squeezed states into cat states [29]; binomial states into GKP states [49]; superposition of vacuum and single-photon state into arbitrary non-Gaussian states [50]; from photon-subtracted squeezed state into arbitrary non-Gaussian states [51]; from two copies of a cubic phase state to a cubic phase state with higher cubicity [23]. For our analysis, we focus on a specific Gaussian conversion protocol of a trisqueezed state to a cubic phase state from [28], for which Gaussian conversion fidelity and success probability are easily available.

In Fig. 6, we present the no-go region for the conversion from a trisqueezed state to a cubic phase state. Again, we notice a lower bound of the error that is independent of the success probability. If we zoom in, we see that the conversion protocol in [28] is very close to the no-go region. The bound we derived here is thus fairly tight to an achievable and known conversion that has experimental relevance.

We leave a detailed assessment of other Gaussian conversion protocols to future work.

## 6 Conclusion

In this work, we have introduced the notion of approximate stellar rank, a robust and operational measure of non-Gaussianity for CV quantum states which generalises the stellar rank and

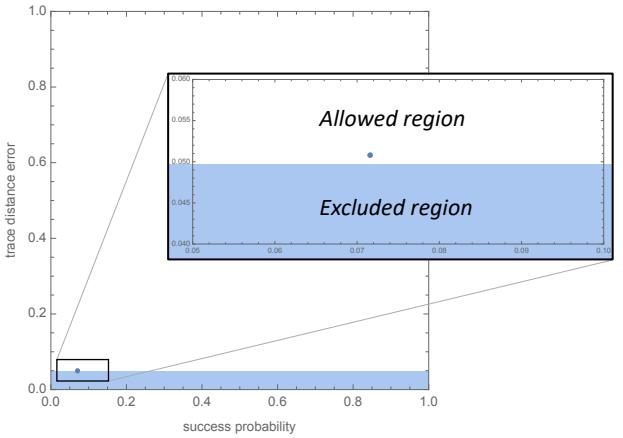


Figure 6: Performance of a Gaussian conversion protocol from a trisqueezed state to a cubic phase state. The blue rectangle is the no-go region for approximate and probabilistic conversion predicted by the approximate stellar rank. The blue point corresponds to the protocol specs. The protocol being assessed is the one from [28, third line in Table III], where the input tri-squeezed state has a triplicity of 0.15.

that is easy to compute in most practical scenarios. We showed that this new measure is a non-Gaussian monotone and leads to a family of bounds for Gaussian conversion, both in the exact and approximate settings, including also probabilistic protocols. These bounds directly imply new no-go results for Gaussian conversion. Moreover, we showed how they can be used to assess the quality of Gaussian conversion protocols, by studying existing protocols. We see that the bound we provide for the conversion between trisqueezed state to cubic phase state studied in [28] is very tight to the reported probabilistic protocol. Thus using our machinery allows to assess experimental relevant and achievable conversion protocols.

Our results have broad applications for quantum state engineering in the CV setting. They reveal the non-Gaussian structure of CV quantum states via profiles of stellar fidelities and make sense of states of infinite stellar rank. The machinery developed in this manuscript allows to assess Gaussian conversion in a very general setting. Moreover, our work opens up for several follow-up directions. These include benchmarking other existing Gaussian conversion protocols against the bounds stemming from the approximate stellar ranks and consequent excluded regions; general-

ising our framework to hybrid protocols where some gates or measurements are non-Gaussian, e.g., by bringing all non-Gaussianity to the input; finally, a further promising avenue for future research is generalising the computational interpretation of stellar rank [43] to the approximate stellar rank, i.e., deriving an approximate classical simulation algorithm of bosonic quantum computations whose computational cost scales with the approximate stellar rank of the computation.

## Acknowledgements

U.C. acknowledges interesting discussions with P. Stornati, F. Centrone, F. Grosshans, S. Mehraabani, R. Nehra, M. Walschaers, H. Yamasaki and R. Takagi. U.C., A.F. and G.F. acknowledge funding from the European Union’s Horizon Europe Framework Programme (EIC Pathfinder Challenge project Veriquib) under Grant Agreement No. 101114899. G.F. acknowledges financial support from the Swedish Research Council (Vetenskapsrådet) through the project grant DAIQUIRI. G.F. and O.H. acknowledge support from the Knut and Alice Wallenberg Foundation through the Wallenberg Center for Quantum Technology (WACQT). O.H. acknowledges the support from CREST Grant Number JP-MJCR23I3, Japan.

## References

- [1] E. Chitambar and G. Gour, “Quantum resource theories,” *Rev. Mod. Phys.* **91**, 025001 (2019).
- [2] S. Lloyd and S. L. Braunstein, “Quantum computation over continuous variables,” in *Quantum Information with Continuous Variables*, pp. 9–17. Springer, 1999.
- [3] N. C. Menicucci, P. Van Loock, M. Gu, C. Weedbrook, T. C. Ralph, and M. A. Nielsen, “Universal quantum computation with continuous-variable cluster states,” *Physical Review Letters* **97**, 110501 (2006).
- [4] C. Weedbrook, S. Pirandola, R. García-Patrón, N. J. Cerf, T. C. Ralph, J. H. Shapiro, and S. Lloyd, “Gaussian quantum information,” *Reviews of Modern Physics* **84**, 621 (2012).
- [5] O. Pfister, “Continuous-variable quantum computing in the quantum optical frequency comb,” *Journal of Physics B: Atomic, Molecular and Optical Physics* **53**, 012001 (2019).
- [6] K. Fukui and S. Takeda, “Building a large-scale quantum computer with continuous-variable optical technologies,” *J. Phys. B: At. Mol. Opt. Phys.* **55**, 012001 (2022).
- [7] B. M. Terhal, J. Conrad, and C. Vuillot, “Towards scalable bosonic quantum error correction,” vol. 5. *Institute of Physics Publishing*, Oct., 2020.
- [8] A. L. Grimsmo and S. Puri, “Quantum Error Correction with the Gottesman-Kitaev-Preskill Code,” *PRX Quantum* **2**, 020101 (2021).
- [9] A. Joshi, K. Noh, and Y. Y. Gao, “Quantum information processing with bosonic qubits in circuit QED,” *Quantum Science and Technology* **6**, 033001 (2021).
- [10] W. Cai, Y. Ma, W. Wang, C.-L. Zou, and L. Sun, “Bosonic quantum error correction codes in superconducting quantum circuits,” *Fundamental Research* **666** (2021).
- [11] V. V. Albert, “Bosonic coding: introduction and use cases,” [arXiv:2211.05714](https://arxiv.org/abs/2211.05714).
- [12] A. J. Brady, A. Eickbusch, S. Singh, J. Wu, and Q. Zhuang, “Advances in bosonic quantum error correction with Gottesman–Kitaev–Preskill Codes: Theory, engineering and applications,” *Progress in Quantum Electronics* **100496** (2024).
- [13] A. Ferraro, S. Olivares, and M. G. A. Paris, “Gaussian States in Quantum Information,” [arxiv:quant-ph/0503237](https://arxiv.org/abs/quant-ph/0503237).
- [14] G. Adesso, S. Ragy, and A. R. Lee, “Continuous variable quantum information: Gaussian states and beyond,” *Open Systems & Information Dynamics* **21**, 1440001 (2014).
- [15] M. Walschaers, “Non-Gaussian quantum states and where to find them,” *PRX quantum* **2**, 030204 (2021).
- [16] S. D. Bartlett, B. C. Sanders, S. L. Braunstein, and K. Nemoto, “Efficient Classical Simulation of Continuous Variable Quantum Information Processes,” *Physical Review Letters* **88**, 097904 (2002).
- [17] A. Mari and J. Eisert, “Positive Wigner Functions Render Classical Simulation of

- Quantum Computation Efficient,” *Phys. Rev. Lett.* **109**, 230503 (2012).
- [18] V. Veitch, N. Wiebe, C. Ferrie, and J. Emerson, “Efficient simulation scheme for a class of quantum optics experiments with non-negative Wigner representation,” *New J. Phys.* **15**, 013037 (2013).
- [19] S. D. Bartlett, B. C. Sanders, S. L. Braunstein, and K. Nemoto, “Efficient Classical Simulation of Continuous Variable Quantum Information Processes,” *Phys. Rev. Lett.* **88**, 097904 (2002).
- [20] S. Rahimi-Keshari, T. C. Ralph, and C. M. Caves, “Sufficient Conditions for Efficient Classical Simulation of Quantum Optics,” *Phys. Rev. X* **6**, 021039 (2016).
- [21] A. Kenfack and K. Życzkowski, “Negativity of the Wigner function as an indicator of non-classicality,” *Journal of Optics B: Quantum and Semiclassical Optics* **6**, 396 (2004).
- [22] F. Albarelli, M. G. Genoni, M. G. Paris, and A. Ferraro, “Resource theory of quantum non-Gaussianity and Wigner negativity,” *Physical Review A* **98**, 052350 (2018).
- [23] R. Takagi and Q. Zhuang, “Convex resource theory of non-Gaussianity,” *Phys. Rev. A* **97**, 062337 (2018).
- [24] U. Chabaud, D. Markham, and F. Grosshans, “Stellar representation of non-Gaussian quantum states,” *Physical Review Letters* **124**, 063605 (2020).
- [25] U. Chabaud and S. Mehraban, “Holomorphic representation of quantum computations,” *Quantum* **6**, 831 (2022).
- [26] L. c. v. Lachman, I. Straka, J. Hloušek, M. Ježek, and R. Filip, “Faithful Hierarchy of Genuine  $n$ -Photon Quantum Non-Gaussian Light,” *Phys. Rev. Lett.* **123**, 043601 (2019).
- [27] O. Hahn, R. Takagi, G. Ferrini, and H. Yamasaki, “Classical simulation and quantum resource theory of non-Gaussian optics,” 2024.  
<https://arxiv.org/abs/2404.07115>.
- [28] Y. Zheng, O. Hahn, P. Stadler, P. Holmvall, F. Quijandría, A. Ferraro, and G. Ferrini, “Gaussian Conversion Protocols for Cubic Phase State Generation,” *PRX Quantum* **2**, 010327 (2021).
- [29] O. Hahn, P. Holmvall, P. Stadler, G. Ferrini, and A. Ferraro, “Deterministic Gaussian conversion protocols for non-Gaussian single-mode resources,” *Phys. Rev. A* **105**, 062446 (2022).
- [30] C. Weedbrook, S. Pirandola, R. García-Patrón, N. J. Cerf, T. C. Ralph, J. H. Shapiro, and S. Lloyd, “Gaussian quantum information,” *Rev. Mod. Phys.* **84**, 621–669 (2012).
- [31] J. Eisert and M. B. Plenio, “Conditions for the Local Manipulation of Gaussian States,” *Phys. Rev. Lett.* **89**, 097901 (2002).
- [32] J. Fiurášek, “Gaussian Transformations and Distillation of Entangled Gaussian States,” *Phys. Rev. Lett.* **89**, 137904 (2002).
- [33] G. Giedke and J. Ignacio Cirac, “Characterization of Gaussian operations and distillation of Gaussian states,” *Phys. Rev. A* **66**, 032316 (2002).
- [34] J. Niset, J. Fiurášek, and N. J. Cerf, “No-Go Theorem for Gaussian Quantum Error Correction,” *Phys. Rev. Lett.* **102**, 120501 (2009).
- [35] R. I. Booth, U. Chabaud, and P.-E. Emeriau, “Contextuality and Wigner Negativity Are Equivalent for Continuous-Variable Quantum Measurements,” *Phys. Rev. Lett.* **129**, 230401 (2022).
- [36] U. Chabaud, G. Ferrini, F. Grosshans, and D. Markham, “Classical simulation of Gaussian quantum circuits with non-Gaussian input states,” *Physical Review Research* **3**, 033018 (2021).
- [37] Y. Yao, F. Miatto, and N. Quesada, “Riemannian optimization of photonic quantum circuits in phase and Fock space,” *SciPost Physics* **17**, 082 (2024).
- [38] I. E. Segal and G. W. Mackey, “Mathematical problems of relativistic physics,” vol. 2. American Mathematical Soc., 1963.
- [39] V. Bargmann, “On a Hilbert space of analytic functions and an associated integral transform part I,” *Communications on pure and applied mathematics* **14**, 187–214 (1961).
- [40] R. Filip and L. Mišta Jr, “Detecting quantum states with a positive Wigner function beyond mixtures of Gaussian

- states,” *Physical Review Letters* **106**, 200401 (2011).
- [41] U. Chabaud, G. Roeland, M. Walschaers, F. Grosshans, V. Parigi, D. Markham, and N. Treps, “Certification of Non-Gaussian States with Operational Measurements,” *PRX Quantum* **2**, 020333 (2021).
- [42] J. Fiurášek, “Efficient construction of witnesses of the stellar rank of nonclassical states of light,” *Optics Express* **30**, 30630–30639 (2022).
- [43] U. Chabaud and M. Walschaers, “Resources for bosonic quantum computational advantage,” *Physical Review Letters* **130**, 090602 (2023).
- [44] O. Hahn and U. Chabaud, “Stellar fidelities and No-go regions.” GitHub repository containing the numerical tools developed for this article.
- [45] A. Ourjoumtsev, H. Jeong, R. Tualle-Brouri, and P. Grangier, “Generation of optical ‘Schrödinger cats’ from photon number states,” *Nature* **448**, 784 (2007).
- [46] J. Etesse, R. Blandino, B. Kanseri, and R. Tualle-Brouri, “Proposal for a loophole-free violation of Bell’s inequalities with a set of single photons and homodyne measurements,” *New Journal of Physics* **16**, 053001 (2014).
- [47] D. J. Weigand and B. M. Terhal, “Generating grid states from Schrödinger-cat states without postselection,” *Phys. Rev. A* **97**, 022341 (2018).
- [48] K. Takase, F. Hanamura, H. Nagayoshi, J. E. Bourassa, R. N. Alexander, A. Kawasaki, W. Asavanant, M. Endo, and A. Furusawa, “Generation of Flying Logical Qubits using Generalized Photon Subtraction with Adaptive Gaussian Operations,” [arxiv:2401.07287](https://arxiv.org/abs/2401.07287).
- [49] Y. Zheng, A. Ferraro, A. F. Kockum, and G. Ferrini, “Gaussian conversion protocol for heralded generation of generalized Gottesman-Kitaev-Preskill states,” *Phys. Rev. A* **108**, 012603 (2023).
- [50] J. Etesse, B. Kanseri, and R. Tualle-Brouri, “Iterative tailoring of optical quantum states with homodyne measurements,” *Opt. Express* **22**, 30357–30367 (2014).
- [51] F. Arzani, N. Treps, and G. Ferrini, “Polynomial approximation of non-Gaussian unitaries by counting one photon at a time,” *Phys. Rev. A* **95**, 052352 (2017).
- [52] L. Lami, B. Regula, R. Takagi, and G. Ferrari, “Framework for resource quantification in infinite-dimensional general probabilistic theories,” *Physical Review A* **103**, 032424 (2021).
- [53] P. V. Parellada, V. G. i Garcia, J. J. Moyano-Fernández, and J. C. Garcia-Escartin, “No-go theorems for photon state transformations in quantum linear optics,” *Results in Physics* **54**, 107108 (2023).
- [54] T. Matsuura, H. Yamasaki, and M. Koashi, “Equivalence of approximate Gottesman-Kitaev-Preskill codes,” *Physical Review A* **102**, 032408 (2020).
- [55] A. J. Pizzimenti and D. Soh, “Optical Gottesman-Kitaev-Preskill Qubit Generation via Approximate Squeezed Schrödinger Cat State Breeding,” [arXiv:2409.06902](https://arxiv.org/abs/2409.06902).
- [56] D. S. Mitrinovic and P. M. Vasic, “Analytic inequalities,” vol. 61. Springer, 1970.
- [57] A. Rastegin, “A lower bound on the relative error of mixed-state cloning and related operations,” *Journal of Optics B: Quantum and Semiclassical Optics* **5**, S647 (2003).
- [58] U. Chabaud, T. Douce, F. Grosshans, E. Kashefi, and D. Markham, “Building Trust for Continuous Variable Quantum States,” in *15th Conference on the Theory of Quantum Computation, Communication and Cryptography*. 2020. [arXiv:1905.12700](https://arxiv.org/abs/1905.12700).

# Appendix

## A Properties of the approximate stellar rank

In this section, we prove the properties of the  $\epsilon$ -approximate stellar rank stated in the main text.

**Proof of Theorem 1.** We show that the  $\epsilon$ -approximate stellar rank (i) vanishes for Gaussian states, (ii) is non-increasing under Gaussian maps, (iii) is monotone on average and (iv) is operationally monotone on average.

(i) The  $\epsilon$ -approximate stellar rank vanishes for Gaussian states:

Given a mixture of Gaussian states  $\rho$ , we have  $r_0^*(\rho) = r^*(\rho) = 0$  and since the  $\epsilon$ -approximate stellar rank is a non-increasing non-negative function this gives  $r_\epsilon^*(\rho) = 0$  for all  $0 \leq \epsilon \leq 1$ .

(ii) The  $\epsilon$ -approximate stellar rank is non-increasing under Gaussian maps:

Fix  $0 \leq \epsilon \leq 1$ , a density operator  $\rho$  and a Gaussian completely positive trace-preserving map  $\mathcal{G}$ . We write  $\sigma = \mathcal{G}(\rho)$ . By definition of the  $\epsilon$ -approximate stellar rank, there exists a density operator  $\tau$  such that  $F(\rho, \tau) \geq 1 - \epsilon$  and  $r^*(\tau) = r_\epsilon^*(\rho)$ . Then,

$$F(\sigma, \mathcal{G}(\tau)) = F(\mathcal{G}(\rho), \mathcal{G}(\tau)) \geq F(\rho, \tau) \geq 1 - \epsilon, \quad (43)$$

where we used the fact that the fidelity does not decrease under quantum operations. Hence,

$$r_\epsilon^*(\sigma) \leq r^*(\mathcal{G}(\tau)), \quad (44)$$

by definition of the  $\epsilon$ -approximate stellar rank. Moreover,

$$r^*(\mathcal{G}(\tau)) \leq r^*(\tau) = r_\epsilon^*(\rho), \quad (45)$$

where we used the fact that the stellar rank is non-increasing under Gaussian maps [25]. Together with Eq. (44) this concludes the proof. Note that a similar proof shows that the  $\epsilon$ -smoothed non-Gaussianity of formation is also non-increasing under Gaussian maps.  $\square$

(iii) The  $\epsilon$ -approximate stellar rank is monotone on average:

We consider a Gaussian positive operator-valued measure  $\{\Pi_\lambda\}_\lambda$ , where  $\Pi_\lambda$  are Gaussian operators with  $\int_\lambda d\lambda \Pi_\lambda = \mathbb{I}$ . Given a density operator  $\rho$ , we write  $p(\lambda) = \text{Tr}(\Pi_\lambda \rho)$  and  $\rho_\lambda$  the normalised post-measurement state. The stellar rank is non-increasing under Gaussian measurements [25], so

$$\int_\lambda d\lambda p(\lambda) r^*(\rho_\lambda) \leq \int_\lambda d\lambda p(\lambda) r^*(\rho) = r^*(\rho), \quad (46)$$

i.e., the stellar rank is monotone on average under Gaussian measurements. Since it is also non-increasing under Gaussian maps, it is monotone on average under Gaussian maps. The same argument shows that the  $\epsilon$ -approximate stellar rank is monotone on average under Gaussian maps for all  $\epsilon$ .  $\square$

(iv) The  $\epsilon$ -approximate stellar rank is operationally monotone on average:

The proof is similar to the previous one: we consider a Gaussian positive operator-valued measure  $\{\Pi_i\}_i$ , where  $\Pi_i$  are Gaussian operators with  $\sum_i \Pi_i = \mathbb{I}$ . Given a density operator  $\rho$ , we write  $p_i = \text{Tr}(\Pi_i \rho)$  and  $\rho_i$  the normalised post-measurement state. The stellar rank is non-increasing under Gaussian measurements [25], so

$$\sum_i p_i r^*(\rho_i) \leq \sum_i p_i r^*(\rho) = r^*(\rho), \quad (47)$$

i.e., the stellar rank is operationally monotone on average under Gaussian measurements. Since it is also non-increasing under Gaussian maps, it is operationally monotone on average under Gaussian maps. The same argument shows that the  $\epsilon$ -approximate stellar rank is operationally monotone on average under Gaussian maps for all  $\epsilon$ .  $\square$

This concludes the proof of Theorem 1.  $\blacksquare$

Note that the stellar rank (and thus the  $\epsilon$ -approximate stellar rank) is not convex in general: for instance, the stellar rank of the state  $\frac{1}{2}|0\rangle\langle 0| + \frac{1}{2}|1\rangle\langle 1|$  is equal to 1, while the mixture of the individual stellar ranks is equal to 1/2.

**Proof of Lemma 1.** The lower bound

$$\max_i r_\epsilon^*(\psi_i) \leq r_\epsilon^*\left(\bigotimes_{i=1}^k \psi_i\right), \quad (48)$$

is a direct consequence of the fact that the  $\epsilon$ -approximate stellar rank is non-increasing under partial trace, which was proven above. For the upper bound, we first pick density operators  $\tau_1, \dots, \tau_k$  such that  $F(\tau_i, \psi_i) \geq 1 - \epsilon_i$  and  $r^*(\tau_i) = r_{\epsilon_i}^*(\psi_i)$  for all  $i \in \{1, \dots, k\}$ . We have

$$\begin{aligned} F\left(\bigotimes_{i=1}^k \tau_i, \bigotimes_{i=1}^k \psi_i\right) &= \prod_{i=1}^k F(\tau_i, \psi_i) \\ &\geq \prod_{i=1}^k (1 - \epsilon_i) \\ &\geq 1 - (\epsilon_1 + \dots + \epsilon_k), \end{aligned} \quad (49)$$

using the Weierstrass product inequality [56] in the last line. By definition of the  $\epsilon$ -approximate stellar rank we obtain:

$$r_{|\epsilon|}^*\left(\bigotimes_{i=1}^K \psi_i\right) \leq r^*\left(\bigotimes_{i=1}^k \tau_i\right) \leq \sum_{i=1}^k r^*(\tau_i) = \sum_{i=1}^k r_{\epsilon_i}^*(\psi_i). \quad (50)$$

$\blacksquare$

## B Exact conversion bounds with stellar fidelities

In this section, we prove Lemma 4 from the main text.

By Lemma 3, if  $m$  copies of  $\sigma$  can be obtained from  $k$  copies of  $\rho$  with probability  $p$  using Gaussian operations, then for all  $0 \leq \epsilon \leq 1$ :

$$r_\epsilon^*(\rho^{\otimes k}) \geq p r_\epsilon^*(\sigma^{\otimes m}). \quad (51)$$

Since the approximate stellar rank is integer-valued, this is equivalent to

$$r_\epsilon^*(\rho^{\otimes k}) \leq n \Rightarrow p r_\epsilon^*(\sigma^{\otimes m}) \leq n, \quad (52)$$

for all  $n \in \mathbb{N}$ , or equivalently

$$r_\epsilon^*(\rho^{\otimes k}) \leq n \Rightarrow r_\epsilon^*(\sigma^{\otimes m}) \leq \lfloor n/p \rfloor, \quad (53)$$

for all  $n \in \mathbb{N}$  and all  $0 \leq \epsilon \leq 1$ . Now, by Lemma 2, for all  $n \in \mathbb{N}$  and all  $0 \leq \epsilon \leq 1$ ,

$$r_\epsilon^*(\tau) \leq n \Leftrightarrow 1 - f_n^*(\tau) \leq \epsilon, \quad (54)$$

for any state  $\tau$ , so Eq. (53) rewrites as

$$1 - f_n^*(\rho^{\otimes k}) \leq \epsilon \Rightarrow 1 - f_{\lfloor n/p \rfloor}^*(\sigma^{\otimes m}) \leq \epsilon, \quad (55)$$

for all  $n \in \mathbb{N}$  and all  $0 \leq \epsilon \leq 1$ . This gives  $1 - f_n^*(\rho^{\otimes k}) \geq 1 - f_{\lfloor n/p \rfloor}^*(\sigma^{\otimes m})$  for all  $n \in \mathbb{N}$ , and thus

$$f_n^*(\rho^{\otimes k}) \leq f_{\lfloor n/p \rfloor}^*(\sigma^{\otimes m}), \quad (56)$$

for all  $n \in \mathbb{N}$ .  $\blacksquare$

## C Approximate conversion bounds with approximate stellar rank

In this section we prove Theorem 3 from the main text. Let  $\omega$  be a density operator such that  $D(\omega, \sigma^{\otimes m}) \leq \delta$  and  $\omega$  can be obtained from  $\rho^{\otimes k}$  using Gaussian operations with probability  $p$ . We make use the following result:

**Lemma 5.** *For density operators  $\rho$ ,  $\sigma$  and  $\tau$ , we have*

$$|F(\rho, \tau) - F(\sigma, \tau)| \leq \sqrt{2D(\rho, \sigma)}. \quad (57)$$

Moreover, if  $\rho = \psi$  and  $\sigma = \phi$  are pure states,

$$|F(\psi, \tau) - F(\phi, \tau)| \leq D(\psi, \phi). \quad (58)$$

We first prove Lemma 5. For density operators  $\rho$ ,  $\sigma$  and  $\tau$ , we have [57, Lemma 1]:

$$|F(\rho, \tau) - F(\sigma, \tau)| \leq \sqrt{1 - F(\rho, \sigma)}. \quad (59)$$

By the Fuchs–van de Graaf inequalities,  $1 - \sqrt{F} \leq D$ , so  $\sqrt{1 - F} \leq \sqrt{1 - (1 - D)^2} \leq \sqrt{2D}$ , which concludes the proof for mixed states.

For pure states  $\psi$  and  $\phi$ , we follow the proof from [58, Lemma 1]: we consider the binary POVM  $\{\tau, \mathbb{I} - \tau\}$  and we write  $P_\psi$  and  $P_\phi$  the corresponding probability distributions for the states  $\psi$  and  $\phi$ , respectively. Then,

$$\begin{aligned} \|P_\psi - P_\phi\|_{\text{tvd}} &= \frac{1}{2}(|P_\psi(0) - P_\phi(0)| + |P_\psi(1) - P_\phi(1)|) \\ &= |P_\psi(0) - P_\phi(0)|, \end{aligned} \quad (60)$$

where  $\|\cdot\|_{\text{tvd}}$  denotes the total variation distance, and

$$\begin{aligned} |F(\psi, \tau) - F(\phi, \tau)| &= |\langle \psi | \tau | \psi \rangle - \langle \phi | \tau | \phi \rangle| \\ &= |P_\psi(0) - P_\phi(0)| \\ &= \|P_\psi - P_\phi\|_{\text{tvd}} \\ &\leq D(\psi, \phi), \end{aligned} \quad (61)$$

by the variational definition of the trace distance.  $\square$

Lemma 5 implies that the set  $\{\tau | F(\sigma^{\otimes m}, \tau) \geq 1 - (\epsilon + \sqrt{2\delta})\}$  contains the set  $\{\tau | F(\omega, \tau) \geq 1 - \epsilon\}$ , so

$$\begin{aligned} r_{\epsilon + \sqrt{2\delta}}^*(\sigma^{\otimes m}) &= \min_{\tau, F(\sigma^{\otimes m}, \tau) \geq 1 - (\epsilon + \sqrt{2\delta})} r^*(\tau) \\ &\leq \min_{\tau, F(\omega, \tau) \geq 1 - \epsilon} r^*(\tau) \\ &= r_\epsilon^*(\omega). \end{aligned} \quad (62)$$

With Lemma 3 we have  $r_\epsilon^*(\rho^{\otimes k}) \geq p r_\epsilon^*(\omega)$ , which directly implies the conversion bound together with Eq. (62). The proof is identical when  $\rho = \psi$  and  $\sigma = \phi$  are pure states, by replacing  $\sqrt{2\delta}$  with  $\delta$ .  $\blacksquare$